

Numerical simulations of soil tests emulating ground behaviour beneath super-tall building foundations

Simulations numériques d'essais de sol reproduisant le comportement du sol sous les fondations d'immeubles de grande hauteur

Y. Zhou*, T. Kiriya

Shimizu Institute of Technology, Tokyo, Japan

*y.zhou@shimz.co.jp

ABSTRACT: Recently, the number of super-tall buildings has been increasing in Japan. The soil beneath such buildings undergoes significant unloading in the excavation phase followed by significant loading during construction, with the latter exceeding 1000 kN/m^2 in some cases. Therefore, it has become increasingly important to consider the confining pressure dependency of the soil when predicting rebound and settlement of the bearing ground during construction. In a previous study, the authors presented a new constitutive model for soil where both the confining pressure dependency and strain dependency are considered. The stress–strain relation was defined using hyperbolic function in the deviatoric stress–strain plane, and its applicability was shown through numerical analysis of soil tests of Toyoura sand. In this work, an improved constitutive model based on modified Ramberg-Osgood (RO) model is proposed. Using the improved model, a series of soil tests on three different undisturbed samples taken from the construction site of a super-tall building is numerically simulated. The improved model is able to replicate the stress–strain relationship with a reasonable degree of accuracy.

RÉSUMÉ: Récemment, le nombre de bâtiments très hauts a augmenté au Japon. Le sol sous ces bâtiments subit une décharge importante lors de la phase d'excavation, suivie d'une charge importante pendant la construction, cette dernière dépassant 1000 kN/m^2 dans certains cas. Par conséquent, il est devenu de plus en plus important de prendre en compte la dépendance de la pression de confinement du sol lors de la prédiction du rebond et du tassement du sol porteur pendant la construction. Dans une étude précédente, les auteurs ont présenté un nouveau modèle constitutif pour le sol dans lequel la dépendance de la pression de confinement et la dépendance de la déformation sont prises en compte. La relation contrainte-déformation a été définie à l'aide d'une fonction hyperbolique dans le plan déviatorique contrainte-déformation, et son applicabilité a été démontrée par l'analyse numérique d'essais de sol de sable de Toyoura. Dans ce travail, un modèle constitutif amélioré basé sur le modèle Ramberg-Osgood (RO) modifié est proposé. En utilisant le modèle amélioré, une série d'essais de sol sur trois différents échantillons non perturbés prélevés sur le site de construction d'un immeuble de grande hauteur est simulée numériquement. Le modèle amélioré est capable de reproduire la relation contrainte-déformation avec un degré raisonnable de précision.

Keywords: Super-tall building; ground settlement; triaxial test; numerical modelling; numerical simulation.

1 INTRODUCTION

In recent years, the number of super-tall buildings (i.e., structures over 300 m high) in Japan has been increasing. The soil beneath such buildings undergoes significant unloading during excavation and then significant loading when the structure is built, with the latter exceeding 1000 kN/m^2 in some cases. Maximum local contact pressure can be as high as 1500 kN/m^2 . During the construction process, the stiffness of the bearing ground decreases during the excavation phase before increasing again as the structure is built, due to the confining pressure dependency of soil stiffness. Since the unloading and subsequent loading values are so large, it has become increasingly important to consider the confining pressure dependency of the soil

when predicting the rebound and settlement of the bearing ground for super-tall buildings. This contrasts with the need to consider only the strain dependency of the soil in the case of smaller buildings.

Around the world, settlement analysis for super-tall buildings with this level of self-weight, such as Burj Khalifa in Dubai (Poulos et al., 2008), Shanghai Tower in China (Xiao et al., 2011), and Lotte World Tower in Korea (Sze et al., 2019), has been performed using conventional constitutive models of soil. However, owing to the differing geotechnical conditions, it is unclear whether the same methods can be used for super-tall buildings in Japan. Tamaoki et al. (1993) proposed a method for predicting soil stiffness based on case studies of buildings with weight per unit area

up to 500 kN/m² in Japan. Because the weight of upcoming new super-tall buildings is significantly larger than this, the applicability of this method is questionable.

In a previous study (Zhou et al., 2022a), the authors presented a new constitutive model for geomaterials where both the confining pressure and strain dependency are considered. The stress–strain relation was defined using hyperbolic function in the deviatoric stress–strain plane, and its applicability was demonstrated through numerical analysis of soil tests on Toyoura sand. In this study, an improved constitutive model based on modified Ramberg-Osgood (RO) model (Tatsuoka et al, 1978), which is more versatile in compared to hyperbolic model, is presented. The applicability of the improved model is verified by performing a series of numerical analyses of soil tests previously carried out (Zhou et al., 2022a) on three different undisturbed samples taken from the construction site of a super-tall building, including both sandy and silty samples.

2 CONSTITUTIVE MODEL OF SOIL WITH BOTH CONFINING PRESSURE AND STRAIN DEPENDENCY

A constitutive model is proposed for three-dimensional numerical analysis in which both the confining pressure and strain dependency are considered. To accommodate loading in an arbitrary direction (i.e., regardless of element coordination), the stress–strain relation is defined in the principal stress–strain space. The stress increment is defined separately for its deviatoric and volumetric components, as shown in Figure 1 and Equation 1:

$$d\sigma' = ds + dp' \quad (1)$$

where $d\sigma'$ is the effective stress increment vector, while ds and dp' are its deviatoric and volumetric components, respectively.

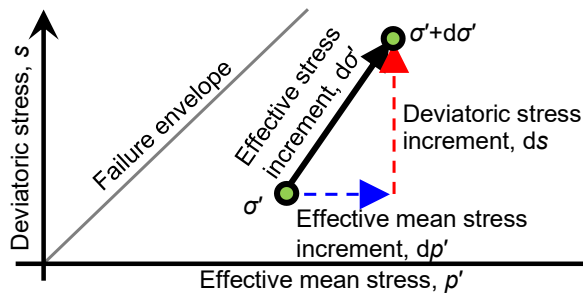


Figure 1. Separation of deviatoric and volumetric components of stress increment.

The skeleton curve of the deviatoric stress–strain ($s \sim \epsilon_{dev}$) relationship, with consideration of both the confining pressure and strain dependency, is given in incremental form by Equation 2:

$$ds = \partial f / \partial p' \cdot dp' + \partial f / \partial \epsilon_{dev} \cdot d\epsilon_{dev} \quad (2)$$

where s (kPa) is deviatoric stress ($=[\sigma'_1 - \sigma'_3]/2$), p' (kPa) is effective mean stress ($=[\sigma'_1 + \sigma'_2 + \sigma'_3]/3$), ϵ_{dev} is deviatoric strain ($=\epsilon_1 - \epsilon_3$), and f is an arbitrary function. In the previous study (Zhou et al., 2022a), hyperbolic function was chosen as a first step. In this study, modified RO model is used because it provides more versatile in replicating the nonlinearity of the soil obtained from laboratory tests. This stress–strain relationship is given by Equations 3–6:

$$\epsilon_{dev} = \frac{h_1 s}{G_0} (1 + \alpha |s|^\beta) \quad (3)$$

$$\alpha = \left(\frac{2}{\epsilon_r G_0} \right)^\beta \quad (4)$$

$$G_0 = G_{0i} \cdot (p'/p'_i)^{n_1} \quad (5)$$

$$\epsilon_r = \epsilon_{ri} \cdot (p'/p'_i)^{n_2} \quad (6)$$

where h_1 is a fitting parameter for the initial stiffness on the skeleton curve, α and β are parameters for the modified RO model, G_0 (kN/m²) is initial shear modulus, G_{0i} and ϵ_{ri} are normalized shear modulus and reference shear strain at unit effective mean stress ($p'_i=1$ kPa), and n_1 and n_2 are parameters for the confining pressure dependency of stiffness and reference shear strain, respectively. By substituting Equations 3–6 into Equation 2, the skeleton curve of the modified RO model is obtained in incremental form as shown in Equation 7:

$$ds = \left[\frac{n_1 s}{p'} + \frac{\alpha \beta n_2 |s|^\beta}{\{1 + \alpha(1 + \beta)|s|^\beta\} p'} \right] \cdot dp' + \frac{G_0}{h_1 \{1 + \alpha(1 + \beta)|s|^\beta\}} \cdot d\epsilon_{dev} \quad (7)$$

The first line in the equation represents confining pressure dependency and the second line represents strain dependency. The skeleton curve of the effective mean stress versus volumetric strain ($p' \sim \epsilon_v$) relationship was not explicitly defined in the previous study. In this study, it is defined as shown in Equations 8 and 9 in incremental form:

$$dp' = K_{0i} \cdot (p'/p'_i)^{n_1} \cdot d\epsilon_v / h_1 \quad (8)$$

$$K_{0i} = 2G_{0i}(1 + \nu) / [3(1 - 2\nu)] \quad (9)$$

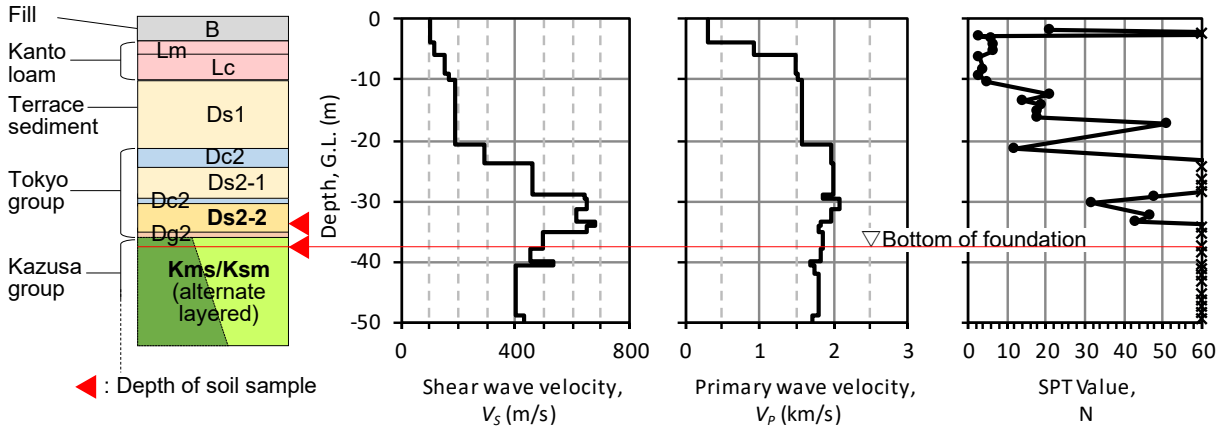


Figure 2. Soil profile of the site where the undisturbed soil samples are taken from.

Table 1. Characteristics of soil samples.

Specimen	Ds2-2	Ksm	Kms
Material	Very dense sand	Consolidated sandy silt	Very dense silty sand
Depth (m)	-33	-37	-37
SPT value, N	32~64	57~100	57~100
Shear wave velocity, V_S (m/s)	600	500	500
Wet density, ρ_t (g/cm ³)	1.68	1.82	1.92
Dry density, ρ_d (g/cm ³)	1.50	1.32	1.51
Cohesion, c_u (kN/m ²)	83	608	85
Internal friction angle, ϕ (deg)	35	20	34

where ε_v is volumetric strain ($=\varepsilon_1+\varepsilon_2+\varepsilon_3$), K_{0i} is normalized bulk modulus at unit effective mean stress ($p'_i=1$ kPa), and ν is Poisson's ratio. As a first step, only the confining pressure dependency is considered in this study.

In the previous study (Zhou et al., 2022a), only the skeleton curve was modelled as a first step. In this study, to accommodate cyclic loading, hysteresis curve is modelled by applying Masing's rule. For simplicity, however, only the strain dependency is considered for the deviatoric component, as shown in Equation 10, while the volumetric component is entirely elastic as shown in Equation 11:

$$ds = \frac{G_0}{h_2 \cdot \left\{ 1 + \alpha(1+\beta) \left| \frac{s}{2} \right|^\beta \right\}} \cdot d\varepsilon_{dev} \quad (10)$$

$$dp' = K_0 \cdot d\varepsilon_v / h_2 \quad (11)$$

$$G_0 = G_{0i} \cdot (p'_{rev}/p'_i)^{n_1} \quad (12)$$

$$K_0 = K_{0i} \cdot (p'_{rev}/p'_i)^{n_1} \quad (13)$$

In these equations, h_2 is the fitting parameter for the initial stiffness on the hysteresis curve and p'_{rev} (kPa) is the effective mean stress at the last unloading point.

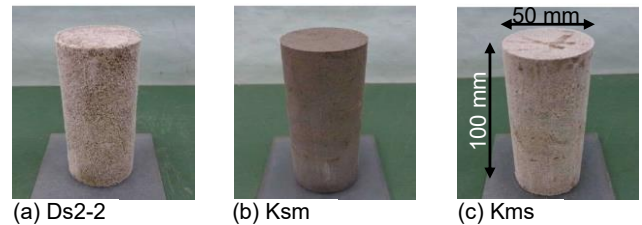


Figure 3. Soil specimens for K0 triaxial tests.

Note that, for Equations 10 and 11, all stresses and strains are given relative to the last unloading point.

3 K0 TRIAXIAL COMPRESSION TESTS OF UNDISTURBED SOIL BENEATH SUPER-TALL BUILDING FOUNDATION

In a previous work, undisturbed soil samples of three different strata were obtained for the purpose of performing K0 triaxial compression tests (Zhou et al., 2022b). The samples were taken using the block sampling method from the construction site of a super-tall building in Tokyo during the excavation phase. Figure 2 shows the soil profile and Table 1 summarizes the characteristics of the sampled soils. The samples consist of two sandy soils (Ds2-2 and Kms) and a silty soil (Ksm) and are all highly dense. The sample soil blocks measured 150 mm in diameter and 150 mm in

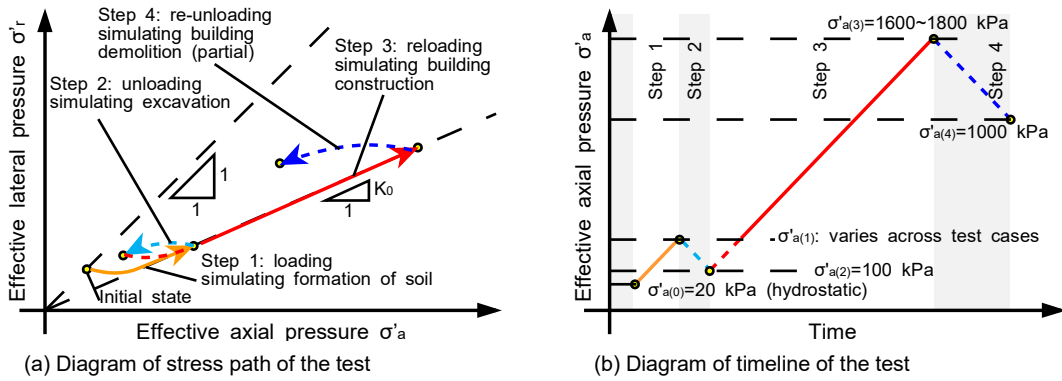


Figure 4. Schematics of stress path and timeline of K_0 triaxial compression tests.

Table 2. List of cases and loading sequence for K_0 triaxial compression tests.

Case ID	Effective axial pressure σ'_a (kPa)			
	(1)	(2)	(3)	(4)
500	500	100	1600 (Ds2-2)	1000
1000	1000		1800 (Ksm, Kms)	
1500	1500			

Table 3. Parameters for numerical simulation of K_0 triaxial compression test.

Parameters		Ds2-2	Ksm	Kms
Normalized shear modulus, G_{0i} (kN/m ²)		23931	88348	15622
Poisson's ratio, ν		0.3	0.3	0.25
Normalized reference shear strain, ϵ_{ri}		7.26×10^{-5}	3.00×10^{-5}	6.11×10^{-5}
Parameter for modified RO model, β		1.506	1.506	1.506
Parameter for confining pressure dependency	Stiffness, n_1	0.483	0.227	0.515
	Reference shear strain, n_2	0.517	0.773	0.485
Fitting parameter for initial stiffness	Skeleton curve, h_1	20	10	10
	Hysteresis curve, h_2	10	5	5

height, from which cylindrical specimens 50 mm in diameter and 100 mm in height were cut out, as shown in Figure 3.

In the series of K_0 triaxial compression tests performed on these specimens, the stress path of soil under a super-tall building foundation during the excavation and construction phases was simulated (Zhou et al., 2022b). Figure 4 shows schematics of the stress path and timeline of the tests. That is, the specimens were subjected to an axial loading and unloading sequence that emulates the stress path the soil undergoes during the construction process. To simulate the boundary condition of the bearing ground, the lateral strain ϵ_r was constrained to zero ($\epsilon_r=0$) by controlling the effective lateral pressure σ'_r , to maintain the specimen in the K_0 condition. The tests were performed by applying incremental axial loading.

Table 2 lists the loading cases and corresponding step-by-step loading sequences. A different axial

pressure $\sigma'_{a(1)}$ was chosen for each case at step 1 to simulate the effective overburden pressure of soil at different depths. Loading case IDs correspond to the value of $\sigma'_{a(1)}$. Each test case is referred to as [name of specimen]-[loading case ID] (e.g., Ds2-2-500). Full test results are presented and discussed in the previous paper (Zhou et al., 2022b).

4 NUMERICAL SIMULATIONS OF K_0 TRIAXIAL COMPRESSION TESTS

Numerical simulations of the K_0 triaxial compression tests described above are performed using the proposed constitutive model to verify its applicability.

Table 3 shows the parameters for the simulations. G_{0i} and n_1 are obtained by measuring the shear wave velocity of the specimens using bender elements during isotropic consolidation tests that were conducted separately, and n_2 is given by $n_2=1-n_1$. ν is

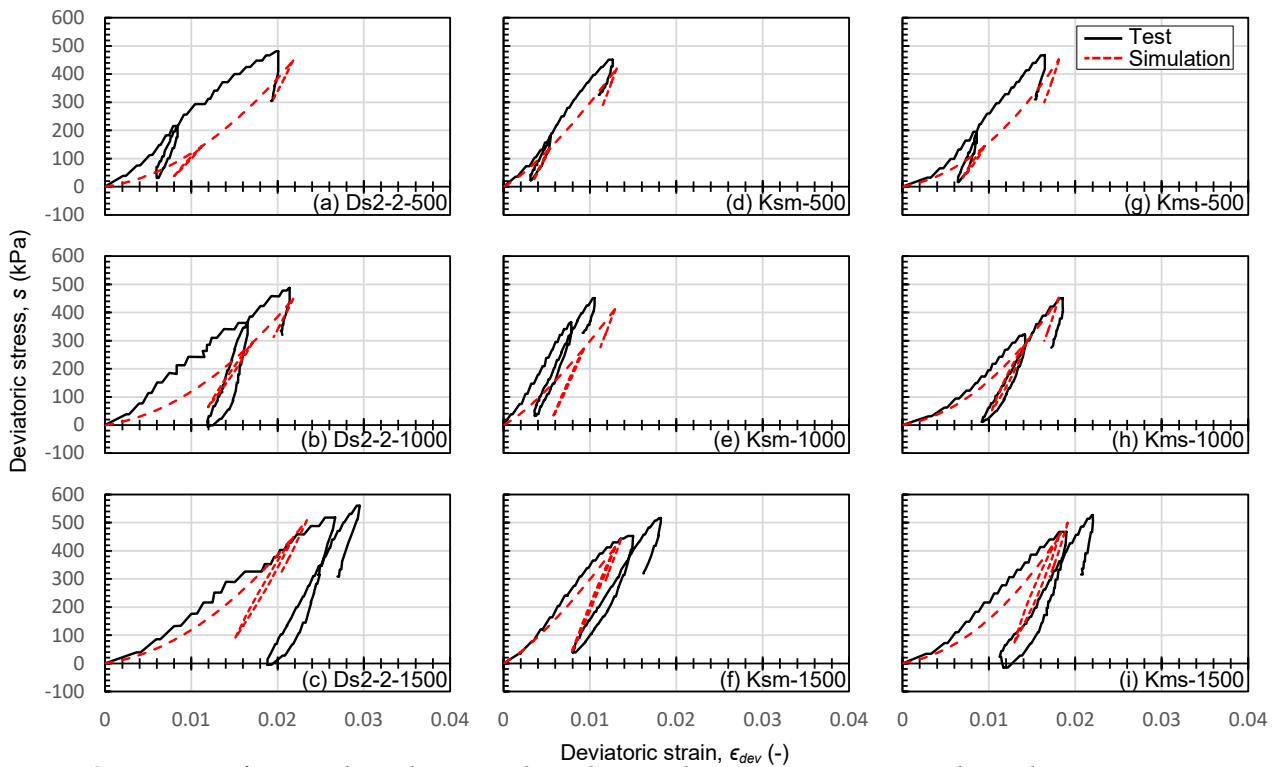


Figure 5. Comparison of test results and numerical simulations: deviatoric stress–strain relationship.

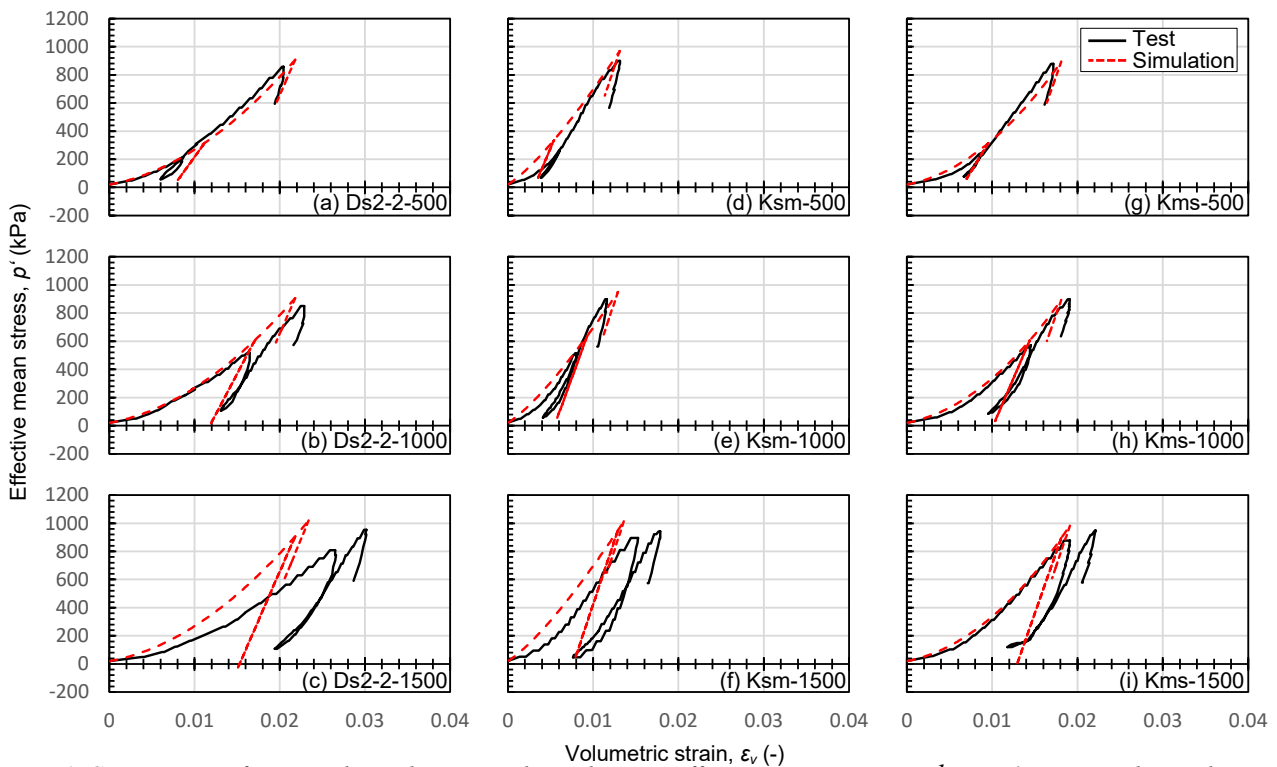


Figure 6. Comparison of test results and numerical simulations: effective mean stress–volumetric strain relationship.

determined from the ratio between the effective lateral and axial stresses (σ'_r/σ'_a) during the K0 triaxial tests (Zhou et al., 2022b). ϵ_{ri} and β are obtained from cyclic shear tests that were conducted separately. h_1 and h_2 are determined by fitting the initial stiffness to the test

results. The lateral boundary is fixed for the simulation, and the same loading sequences as the tests are applied.

Figure 5 shows the deviatoric stress–strain ($s \sim \epsilon_{dev}$) relationships and Figure 6 shows the effective mean stress–volumetric strain ($p' \sim \epsilon_v$) relationships,

comparing the results of the tests and numerical simulations for all cases respectively. (Test results are plotted with black lines and simulation results with red dashed lines.)

In the test results, the skeleton curves of both $s\sim\epsilon_{dev}$ and $p'\sim\epsilon_v$ relationships exhibit notably downward convex curves in all cases, suggesting that the gradually increasing stiffness due to confining pressure dependency has a dominant effect on the stress–strain relationships for all the three samples. As for the $s\sim\epsilon_{dev}$ relationships, the skeleton curves tend to transition to upward convex shapes as the strain increases, forming slightly S-shaped curves overall. The simulations are able to reproduce the downward convex shape of the $p'\sim\epsilon_v$ skeleton curves (Figure 6). Although the simulated $s\sim\epsilon_{dev}$ skeleton curves do not exhibit the S-shape seen in the tests, the stress–strain relationships are in overall good agreement with the test results.

Looking at hysteresis curves, the limitations of the simplistic approach taken in this study mean that the simulated $p'\sim\epsilon_v$ hysteresis is notably linear, as opposed to confinement pressure and strain dependency to a reasonable degree. This suggests that the proposed model has applicability in predicting the rebound and settlement of bearing ground during the construction of super-tall buildings.

Future work for the authors is to modify the modelling of hysteresis curve to improve the reproducibility of unloading and reloading behaviour. The authors also plan to use the proposed constitutive model to analyse the settlement of existing super-tall buildings.

REFERENCES

- Poulos, H. G. and Bunce, G. (2008). Foundation design for the Burj Dubai—the world’s tallest building. In: *Proceedings of 6th Conference of the International Conference on Case Histories in Geotechnical Engineering*, Arlington, VA, 14. Available at: https://scholarmine.mst.edu/icchge/6icchge/session_01/14, accessed 19/10/2023.
- Sze, J. and Lam, A. K. (2019). A Combo Foundation Does the Job: Piled-Raft Foundation Design for a Supertall Skyscraper. *Geo-Strata—Geo Institute of ASCE*, 23(4), pp. 42-49. <https://doi.org/10.1061/geosek.0000152>.
- Tamaoki, K., Katsura, Y., Nishio, S. and Kishida, S. (1993). Estimation of Young’s Moduli of Bearing Soil Strata. In: *Excavation in urban areas: Proceedings of 2nd Kansai international geotechnical forum on comparative geotechnical engineering (KIGForum'93)*, pp. 23-33.
- Tatsuoka, F. and Fukushima, S. (1978). 砂のランダム繰返し入力に対する応力～歪関係のモデル化について
- to the overall upward convex shape seen in the test results (Figure 6). Overall, however, the simulations are able to reproduce the cyclic stress–strain relationships as affected by both confinement pressure and strain dependency to a reasonable degree.
- The results demonstrate that the proposed constitutive model has a certain degree of applicability in predicting the rebound and settlement of bearing ground during the construction of super-tall buildings.

5 CONCLUSIONS

A constitutive model is proposed for geomaterials that takes into consideration both confining pressure and strain dependency. This proposed constitutive model, which is based on modified Ramberg-Osgood model, is used to numerically simulate previously reported K0 triaxial compression tests on undisturbed soil samples from the bearing ground of a super-tall building. Overall, the simulations are able to reproduce the cyclic stress–strain relationships as influenced by both

(1) (Stress-Strain Relation of Sand for Irregular Cyclic Excitation (1)). *Journal of Institute of Industrial Science*, The University of Tokyo. 30(9), pp. 356-359. (In Japanese) Available at:

<https://ndlsearch.ndl.go.jp/books/R000000004-I1962092>, accessed 27/02/2024.

Xiao, J. H., Chao, S. and Zhao, X. H. (2011). Foundation design for the Shanghai Center Tower. *Advanced Materials Research*, Vol. 243, pp. 2802-2810. <https://doi.org/10.4028/www.scientific.net/AMR.243-249.2802>.

Zhou, Y. and Kiriyama, T. (2022a). Numerical Implementation of Ground Behaviors Beneath Super-Tall Building Foundations During Construction. In: *Proceedings of 4th International Conference on Performance Based Design in Earthquake Geotechnical Engineering (PBD-IV 2022)*, Beijing, China, pp. 1277-1285. https://doi.org/10.1007/978-3-031-11898-2_108.

Zhou, Y., Kiriyama, T. and Saito, A. (2022b). 超々高層建物基礎下地盤の施工時挙動を再現した要素試験 (Element Tests Simulating the Behavior of Soil under Supertall Building during Construction). In: *Proceedings of 57th Japan National Conference on Geotechnical Engineering*, Niigata, Japan, 20-8-3-2~3 (In Japanese).

INTERNATIONAL SOCIETY FOR SOIL MECHANICS AND GEOTECHNICAL ENGINEERING



This paper was downloaded from the Online Library of the International Society for Soil Mechanics and Geotechnical Engineering (ISSMGE). The library is available here:

<https://www.issmge.org/publications/online-library>

This is an open-access database that archives thousands of papers published under the Auspices of the ISSMGE and maintained by the Innovation and Development Committee of ISSMGE.

The paper was published in the proceedings of the 18th European Conference on Soil Mechanics and Geotechnical Engineering and was edited by Nuno Guerra. The conference was held from August 26th to August 30th 2024 in Lisbon, Portugal.